Industrial lubricant removal using an ultrasonically activated water stream, with potential application for Coronavirus decontamination and infection prevention for SARS-CoV-2

M. Malakoutikhah[1,2]*, C. N. Dolder[1,2], T. J. Secker[3], M. Zhu[1], C. C. Harling[2], C. W. Keevil[3] and T. G. Leighton[1,2]

[1] *Sloan Water Technology Ltd., 1 Venture Road, Chilworth, Southampton, SO16 7NP, United Kingdom*

[2] *Institute of Sound and Vibrations, University of Southampton, Southampton, United Kingdom*

[3] *Biological Sciences, University of Southampton, Southampton, United Kingdom*

E-mail: M.Malakoutikhah@soton.ac.uk

Maryam Malakoutikhah MEng is a Postgraduate Research Student within Engineering and the Physical Sciences at the University of Southampton. Maryam received her Bachelor's degree in Electronics and Telecommunications Engineering from the Azad University, Iran. She obtained her MSc with First Class Honours in Electronic Communications and Computer Engineering from the University of Nottingham in 2014. Inspired by Professor Timothy Leighton's research on bubble acoustics, and having consequently attended the a Global-NAMRIP conference where he spoke in 2015, she decided to pursue a PhD under his supervision, which she began in 2016 on the topic of ultrasonic cleaning. Her PhD is currently sponsored by Sloan Water Technology Ltd.

Craig Dolder PhD is a Senior Scientist at Sloan Water Technology Ltd. He graduated with his PhD in May 2014 from The University of Texas at Austin where he worked for the Applied Research Laboratories researching varied topics including fish school acoustics and turbulent flow noise. Prior to his work at The University of Texas he obtained his BSE in Acoustical Engineering at the University of Hartford. After signing up for the Acoustical Society of America's 'Students meet members for lunch' scheme, he and Professor Leighton were paired for lunch at the 2013 meeting of the Society in Montreal, and he subsequently undertook postdoctoral research in anaerobic digestion within Professor Leighton's ultrasonics team, where he participated in a range of multidisciplinary projects in Global-NAMRIP, including winning funding for several Outreach projects.

Tom Secker PhD is a Research fellow in infection prevention within Biological Sciences in the Faculty of Environmental and Life Sciences. He gained a BSc (Hons) Biomedical sciences in 2006 from Sheffield Hallam University, UK, then his PhD in 2012 on "Cell based prion infectivity assays" at the University of Southampton, UK. He collaborates closely with Professor Leighton's engineering team at the University and undertakes multidisciplinary research as a member of Global-NAMRIP.

Mengyang Zhu PhD is a research engineer at Sloan Water Technology Ltd., UK. Prior to his current role, he undertook a PhD in bubble acoustics under Professor Leighton's supervision at the University of Southampton. He received his Bachelor's and Master's degree in electronic engineering from the Northwestern Polytechnical University, Xi'an, China. His research interests include ultrasonic cleaning and high-speed image analysis.

Christopher Harling CBE FRCP is a former physician and adviser in the Department of Health who, after retirement, took a master's degree in marine biology before starting a part time PhD in Southampton with Prof. Leighton investigating the role of liquid acoustic stream technology in the management of chronic wounds and other related health issues. He has previously served on a number of specialist advisory committees on viral diseases, infectious diseases generally and medical ethics.

Bill Keevil FIBiol FAAM FRSM FRSPH is Professor of Environmental Healthcare at the University of Southampton where he is Director of the Environmental Healthcare Unit. He is Chair of the University of Southampton Genetic Modification and Bio-Safety Committee and Chair of the Government's Advisory Committee on the Microbiological Safety of Food. He is a Fellow of the Royal Society of Biology, Fellow of the American Academy of Microbiology, Fellow of the Royal Society of Medicine, Fellow of the Royal Society for Public Health, and winner of the 1985 Colgate Prize.

Timothy G Leighton, FRS FREng FMedSci ScD is the founder and Chair of the Global Network for AntiMicrobial Resistance and Infection Prevention (Global-NAMRIP). He is Professor of Ultrasonics and Underwater Acoustics at the Institute of Sound and Vibration Research, University of Southampton, UK; and a Director and the Inventor-in-Chief of Sloan Water Technology Ltd., a UK manufacturer and R&D establishment founded on his patents and inventions, including the Ultrasonically Activated Stream (UAS) technology.

Industrial lubricant removal using an ultrasonically activated water stream, with potential application for Coronavirus decontamination and infection prevention for SARS-CoV-2

Industrial processes routinely require the removal of lubricant from processed materials. This cleaning can be energy intensive and environmentally costly owing to the temperatures and the solvent load that are used. It is required throughout many industrial processes, notably surface finishing. This paper tests a novel technology that removes the need to heat the water, and reduces the need for additives, through use of a novel nozzle that uses just mains water and electricity to generate an 'Ultrasonically Activated Stream' (UAS). The UAS nozzle passes ultrasound down a stream of unheated water, and tests its ability to remove a variety of lubricants, from stainless steel, with and without the addition of degreaser, comparing it to the ability of the same water supply (when not ultrasonically activated) to remove the lubricant (with and without degreaser). Removal of the need to heat water by use of this UAS nozzle would reduce heating costs and allow areas of a plant or manufacturer that lack access to hot water to have enhanced cleaning. Reduction in the need to use additives reduces costs and is a requirement for surfaces that may be damaged by them. However, the implications extend further. If, in the current COVID-19 crisis, supply chains for solvents are broken, or additives and heating become difficult to access (for example to decontaminate PPE or an ambulance in the field), the ability to remove lubricant without heating (and, if necessary, additives such as detergents) is crucial, since the SARS-CoV-2 virus resides in respiratory secretions that are composed mainly of mucin glycoproteins, surfactant and intercellular fluid.

Keywords: ultrasonic cleaning, grease, oil, lubricant, cleaning, finishing, joining, bonding, welding, electroplating, COVID-19, Coronavirus, SARS-CoV-2 virus, cavitation, bubble

Introduction

Oils and greases, by their nature, are resistant to removal by room temperature water, so that the use of substantial energy to heat the water, and the addition of detergents, are routine when removing such lubricants. This incurs considerable financial and

environmental costs, for example in electricity consumption [1] and wastewater contamination [2].

Lubricants are persistent viscous materials that attach to surfaces for long periods, used notably to reduce friction and wear [3]. The Minimal Quantity Lubrication (MQL) protocol [4] reflects not only their cost [5] and their environmental and health implications, and but also the importance of cleaning the surfaces to which they attach prior to plating [6], welding [7] and adhesion-bonding [8] and other processes that depend on suitable clean surface preparation [9]. Following the Montreal Protocol, there is a drive to replace the use of pure methyl chloroform or chlorofluorocarbon solvents with aqueous cleaning solutions [10]. This paper investigates the ability of a novel nozzle [11] that emits an 'Ultrasonically Activated Stream' (UAS) of water to remove lubricants from stainless steel using unheated water from the mains, both with and without pre-treatment of the surface with a commercial degreaser (Figure 1). Unheated mains tap water enters an acoustic cone, into which a transducer emits ultrasound [12]. The water and ultrasound issue from the nozzle and, when microscopic air bubbles in the water flow reach the surface to be cleaned, the ultrasound excites surface waves on the walls of the bubbles [13, 14] (shown in expanded view in Figure 1). These surface waves in turn set up microcirculation currents in the liquid that remove contaminants attached to the solid [12]. A particular difficulty that the cone overcomes is the tendency of acoustic energy not to propagate down narrow streams of water, and a particular potency of the technique is the way the sound field interacts with the target to set up radiation forces [15, 16] that draw the bubbles into the crevices that traditional cleaning techniques (brushing, wiping etc.) find difficult to access [16, 17]. The forces exerted by the microcirculation currents are, importantly, in the range that removes the contaminant in question, but insufficient to damage the target (even microscopic scratches could make subsequent cleaning more

difficult, act as dirt traps and niches for microbial colonization, and initiate erosion and corrosion).

The ability to reduce or eliminate the need to use additives (detergents, organic solvents etc.) reduces financial and environmental costs, and would assist for those surfaces that cannot tolerate such additives (e.g. some coated lenses). Furthermore, the ability to remove lubricants from surfaces using unheated mains tap water through this UAS nozzle would facilitate enhanced cleaning in areas of a factory, or product component, that do not have access to a flow of hot water, and reduce the financial and environmental costs of heating water. Indeed, the mains tap water in this study was used to fill a recirculating portable system (the water being replaced daily) to reduce water wastage and allow the unit to be taken to the requisite area of the lab for testing, which did not itself have access to mains water.

Cleaning of surface contaminants is not restricted to industrial processes. The current COVID-19 pandemic reveals another facet of the need for cleaning, and a role for a UAS nozzle that generates cleaning water that requires no heating and can operate with reduced, or zero, additives. An emerging illness by definition will have no preventive vaccination and no specific treatment. Control of the outbreak relies on non-specific measures to break the chain of transmission of the SARS-CoV-2 virus (which resides in respiratory secretions that are composed mainly of mucin glycoproteins, surfactant and intercellular fluid; Figure 2), of which cleaning of hands and solid surfaces are a vital part. During the early days of a pandemic, supplies of consumables can be jeopardized by broken supply lines, panic buying, and illness amongst staff in the production, warehousing, and delivery sectors. Cleaning regimes come under scrutiny, leading to a greater rate of consumption of these cleaning agents and water. Instructions may even be issued to clean and re-use items formerly considered as disposable (e.g. PPE). Moreover,

installations that are mobile (e.g. ambulances) or in the process of being set up (mobile hospitals, clinics and mortuaries) can take time to establish access hot water and sufficient stocks of bleach and detergents etc). The portable UAS nozzle, operating on the minimal requirements these facilities need (electricity and water), which if appropriate can operate free of the reliance on chemical consumables and *in extremis* even able to operate using portable or recirculating water systems, offers opportunities to access good cleaning in such difficult circumstances.

We have previously shown the ability of UAS nozzle to remove contaminants in a range of applications, including cleaning baby equipment [11], hands [12], foodstuffs and associated pipework/packaging [11, 17, 18], rail components [12, 19], surgical instruments [20] and tools [12], grease [12], bone prior to transplant [20], and dental [20, 21] and marine [22] biofilms. The effective tackling of biofilms using only sound, air and water meant that, unlike the use of conventional antimicrobial treatments (antibiotics, antivirals, antifungals etc.), the use of such technology should not so readily promote the rise of AntiMicrobial Resistance (AMR) [18, 23, 24].

In this paper, we demonstrate the ability to remove industrial lubricants to add to the list of surface contaminants that can be removed by this technology and discuss some of the implications for cleaning methods.

Overview of bubble-based cleaning methods

Several detergent-free methods exploit bubbles in full or partial place of detergents. One technique submerges contaminated objects into a bath and subjects them to an underwater highspeed jet of hot water (similar to a ‘jacuzzi’) [25]. Microbubbles in the bath can passively assist in removing oil and grease without the use of detergent because the hydrophobic nature of these lubricants, coupled with a mechanical action of the hot jet,

can cause the oil and grease to collect at the interface with gas (usually air) at the bubble wall [25]. The slow buoyant rise speed of microbubbles gives them time to collect oil and grease from bodies of water [26]. Such an approach has limited success, depending on the type and load of contaminant [27].

The mechanical action of the hot water jet pool can be replaced by inertial cavitation if the oil/grease-contaminated object is placed in an ultrasonic cleaning bath [28]. Ultrasonic bath treatment has been satisfactory for many surface tolerances for decades [29], although tolerances, and the size of particles that require removal, tend to become finer over time [30, 31]. In this context, inertial cavitation is a physically damaging activity [32] , generating free radicals [33, 34] and blast waves [35]. Whilst this is a useful action for removal of contaminants, it can lead to pitting and erosion in the target being cleaned [36-39]. This makes repeat cleaning by inertial cavitation more difficult as scratches and other defects in the surface finish, that were induced by previous cleans, provide crevices from which contaminants are more difficult to remove in subsequent cleans, and act as sources of wear and corrosion. Furthermore, as with all treatments that require submersion, items too large to fit in the ultrasonic cleaning bath cannot be treated, items cannot be ‘cleaned in place’, and the necessity for submersion means that the target being cleaned can be re-contaminated by material previously removed from it or a preceding/neighbouring sample [11]. Moreover, the sound field in an ultrasonic cleaning bath is highly inhomogeneous, such that some regions (‘hot spots’) are over-treated and can be damaged, whilst some regions (‘cold spots’) lack cavitation and remain uncleaned [40, 41]. Furthermore, immersion of a sample in an ultrasonic bath can significantly degrade the sound field, emphasizing the problem of ‘cold’ and ‘hot’ spots [42] (Figure 3).

This paper reports on the first testing of lubricant cleaning by an ultrasonic method that overcomes these difficulties. It does this by generating a well-defined acoustic field at the base of a stream of water, which rinses away contaminant, so preventing re- and cross-contamination, and allowing items to be cleaned in place. Furthermore, it uses a form of bubble activity that is qualitatively different from inertial cavitation [43], leading to far less surface damage.

This new form of cleaning followed from Leighton's discovery of a previously unobserved ultrasonic signal in the 1980s [44]. He identified its cause as ultrasonically-induced surface waves on the bubble wall [15, 45] (Figure 4). This led to a new method of ultrasonic cleaning by identifying the method to stimulate and control those waves [13, 14] and couple them to Bjerknes forces [15, 16, 46] to cause the bubbles hosting those waves to be forced into any cracks and crevices in a solid [17]. This particularly important, because the local convection currently and shear created by these surface waves [15, 43], as they ripple across the bubble wall, are able to remove sticky and particulate contaminants from such crevices (Figure 5).

An example of this type of behaviour is shown in Figure 5, where a sticky contaminant is placed on a submerged block of glass, into which a cylindrical pore about the diameter of a mid-size human hair has been etched (Figure 5(a)). At the base of this pore is a sensor which records, by the graph shown at the base of each panel, how clean the base of the pore is. The red vertical line on the graph indicates the time corresponding to the movie frame above it. The contaminant layer is stable before the ultrasound is turned on (Figure 5(a)) but is rapidly removed from the flat upper surface of the glass when the ultrasound is turned on, making the water cloudy (Figure 5(b)).

However, the electrode shows that the base of the pore is still dirty in Figure 5(b). Driven by Bjerknes forces, bubbles hosting surface waves (just visible in the pore in

Figure 5(b)), have automatically found and entered the pore, but they have not made their way yet to the base. Because the bubbles have not reached the base of the pore, the electrode shows that the base of the pore is still dirty in Figure 5(b); this remains the case until the moment the bubbles reach the bottom of the pore (Figure 5(c)) at which point they clean it (Figure 5(d)) and the electrode signal shows the pore to be clean.

However in order to deliver both the microbubbles, and the ultrasound that excited surface waves on their walls, down a stream of water to the target to be cleaned (Figure 1), Leighton needed to address the losses and scattering that would occur in streams of water surrounded by pressure-release acoustic boundaries [47, 48] with acoustic pulsing [15, 49-52].

Methodology

Four different cleaning conditions were tested. Tokens were cleaned with water flowing through the UAS nozzle without ultrasonic enhancement. Tokens were cleaned with the UAS on. Subsequently, both cases were repeated with a degreasing agent that was applied 30 minutes prior to the treatment with water (and, where relevant, ultrasound). Whilst the UAS device normally runs directly from the water mains, the desire to conserve water prompted use of a portable recirculating water system, which produced the added benefit of allowing experiments in a laboratory location that did not have access to mains water. The recirculating water system was refilled with fresh mains water each day, and contained two filters to reduce the contamination that re-entered the device via recirculation.

Four lubricants were chosen to cover a wide range of viscosities (lacking equipment to measure these, literature- or manufacturer-values were quoted, although of course these are not at the temperature tested). The least viscous lubricant tested was

Sunflower oil (cited [53] to have a viscosity at 40°C is 0.0316 Pa s). The second most viscous lubricant was a synthetic Poly-alpha-olefin (PAO) grease (brand name Special Plastic Grease, SPG) with a published viscosity of 0.041 Pa s at 40°C [54]. The third lubricant was a refined mineral oil based (MO) grease (brand name Sapphire 2) and is cited [55] to have a viscosity at 40°C of approximately 0.162 Pa s. The fourth lubricant was silicone grease, which is reported [56] at 40°C to have a viscosity of 0.65 Pa s. A commercial degreasing agent (DA, named heavy-duty three-in-one foaming spray with active agents limonene, butoxyethanol, and isopropyl alcohol) was used in those tests requiring it. Each material and experimental case was repeated five times, leading to a total of 80 individual tests.

Stainless steel tokens measuring 10 mm by 10 mm by 1 mm thick were bonded to acrylic plates for handling. Without this bonding, handling of the token (to take it to the weighing and imaging sensors) could perturb the lubricant loading to an unacceptable extent. Bonding to acrylic overcame this, but came at the cost that lubricant removed from the steel by cleaning could be relocated onto the acrylic and still count towards the post-cleaning mass value. This was deemed acceptable because: (i) the use of imaging would always log this phenomenon; and (ii) such ‘sideways’ relocation of lubricant should not be ignored, as it represents a cleaning action that does not remove the lubricant and take it into solution to be transported away from the metal, but rather produces mountains and grooves in the lubricant layer (and if metal samples were contiguous, would shift lubricant from one onto another).

Once the steel was bonded to an acrylic base, a 1.6 mm template plate with a 10 mm by 10 mm hole was placed over the steel token. The 0.6 mm gap above the steel token was filled with lubricant and then levelled off (by sliding a thin glass-slide on top of the gap as shown in Figure 6) with a straight edge, leaving a suitably uniform layer of

lubricant on the token. For the subset of tokens being measured with a degreaser, the degreaser was sprayed into a reservoir so that a pipette could be used to apply 0.05 ml of the product to the coated token. The tokens were then allowed to sit for 30 minutes before being cleaned.

Two methods were used to characterize the amount of lubricant on each token, before and after cleaning. Weighing provides a rapid 3D assessment, but without spatial resolution on the inhomogeneity of cleaning of a particular token. Consequently, it provides no insights as to the mechanism for lubricant removal. In contrast, microscopy is able to reveal inhomogeneity in cleaning, but is very time-consuming. It is in principle a 2D method; here it was made 3D by introducing a method to exploit depth-of-field limitations to provide an advantage, specifically to map the thickness of lubricant. However, this could only be done for the two contaminants, PAO and the MO lubricant, since the other two lubricants (sunflower oil and silicon grease) were too translucent for this method.

The procedure for estimating the mass of lubricant removed is as follows. The steel tokens and the acrylic base plates were bonded together then weighed together. After that, a layer of lubricant was deposited as described above. The mass of the base plate, token, surrounding acrylics and lubricant was then recorded, allowing the mass of lubricant deposited on each token (and on the acrylic surround) to be assessed.

The tokens were cleaned as shown in Figure 1. The distance between the nozzle and the token was held at 10±2 mm and the flowrate was held at 2±0.2 L/min for 2 minutes. The stream was oriented perpendicular to the tokens. The temperature of the water was 22±2 °C. After cleaning, the samples were left to dry for 24 hours at room temperature and then re-weighed.

A second set of measurements was conducted using the PAO and the MO lubricant. Visualisation of the grease on the stainless steel tokens was carried out using sensitive Episcopic Differential Interference Contrast (EDIC) microscopy (Nikon Eclipse LV100, custom modified by Best Scientific, UK [57, 58]). The EDIC microscope takes the fundamentals of Nomarski DIC (Differential Interference Contrast) but using episcopic light as opposed to the transmitted light of Nomarski DIC. This allows the visualisation of translucent samples directly on opaque surfaces, creating a pseudo-3D image of the sample with high resolution, in the z-plane. Long Working Distance (LWD) lenses utilised with EDIC microscopy allows samples to be visualised with minimal sample preparation [57].

In brief, the principle of this optical measurement was that a microscope would be focused onto the token surface where it was visible, which was then used as a datum when the microscope was subsequently focused onto the surface of the lubricant (Figure 7). Many images of the type shown in Figure 7 were stitched together to form images of the whole token (Figure 8), but at far higher resolution than could be obtained by simply photographing the token. The resolution of the microscope images of the type shown in Figure 7 is 0.96 μm/px, which allows detailed visualization of the deformation of the lubricant remaining after cleaning, and hence indicate something of the mechanism for removal (section 3).

Optical measurements allow an assessment of how the lubricant is moved from one part of a given tile to another part of it, and the extent to which it is removed from the tile entirely, and whether it is moved onto the acrylic surround or removed into the liquid – a slower but more sophisticated measurement than that of the total mass removed. The cleaning method proceeded exactly as above. To detail the process introduced above, the slides were imaged under a microscope before (Figure 8(a)) and after (Figure 8(b))

cleaning. Each tile had a portion of the lubricant removed (circled in the top left corner of Figure 8(a)) to provide a baseline datum for the top of the steel, and to calibrate the height of the lubricant (which varied over the sample). The imaging microscope has a calibrated height axis. For each image of the type shown in Figure 8, the microscope was focused on the surface of the lubricant and the height of that image was recorded. An initial sensitivity test (that excluded the image that had been cleaned to provide a datum) showed that the deviation of heights within one image had a standard deviation of 0.005 mm. The flatness of the bare token and its horizontal alignment produced smaller errors than this. Therefore, the error due to height variation within each image was considered insignificant and the height of each image was measured only once when the maximum amount of surface was in focus. This method resulted in detection of the lubricant height at 80 different points for each token (shown in Figure 8(c)) for both before and after cleaning. If there was an area where the tile surface was clean, an additional photo was taken of the tile surface.

For each of the panels of Figure 8 (and each corresponding repeat of each tested sample of each lubricant), 80 images (plus any focused on the tile surface) were stitched together to form a complete image of the tile. By attributing a single mean lubricant height (Figure 8(c&d)) to each of the 80 sub-areas (measuring 1340 μm×1000 μm each), the original fine resolution of the microscopy is reduced to provide an estimate of the volume of the lubricant on the tile before and after cleaning. The images were thresholded to determine the percentage of the area cleaned of lubricant as shown in Figure 8(e&f).

Results

The high-resolution microscope images allow detailed visualization of grooves and ridges formed in the lubricant by bubbles (Figure 9). These formations suggest a burrowing

mechanism (in keeping with theory [16]), whereby the Bjerknes forces drive the bubbles through the lubricant towards the steel. Having penetrated the lubricant surface, liquid can be pumped (by the surface waves), from the liquid above the lubricant down to the bubble, lifting the lubricant from the steel surface. The images suggest this is a more likely mechanism for lubricant removal than uniform erosion of the lubricant layer by the bubbles from above.

Figure 9b shows the necessity of conducting the optical measurement method, because even though the lubricant is removed from the tokens, it still remains on the acrylic plate, so the weighing method cannot accurately measure the amount of lubricant removed from the surface of the token.

Figure 10 shows the photographic record for a full set of studies on the removal of PAO from a token, indicating that unheated UAS water, with and without degreaser (the latter causing enhanced removal), is effective at displacing the grease. In contrast, the same water without the UAS technology is ineffective at removing the grease, either with or without degreaser. Figure 11 shows the corresponding full set of microscopy images, stacked together to produce a composite image.

Mass measurements

The amount of lubricant removed depended heavily on both the viscosity of the lubricant and the method used. Figure 12 shows the results of the mass removal for each lubricant and removal method. The majority of the sunflower oil was removed in every case, and no significant improvement was seen using either a degreasing agent or UAS. For the PAO grease the amount removed by water alone was negligible and UAS alone was able to remove 12±4% (where all ± figures are the standard error of the mean).

The addition of the DA allowed 7±2% removal and the combination of DA and UAS brought the removal up to 31±8%. The MO based grease was resistant to removal for all cases other than the combination of UAS and DA, which yielded 11±1%. The silicone grease proved difficult to remove under all cases.

The measured mass increased slightly in a few samples due to water not evaporating completely during the 24-hour drying period. Further analysis was done on the two most interesting cases, where the lubricant was not easily removed by all methods (as was the case with sunflower oil) nor did it successfully resist all methods (as did silicone grease). For the two intermediate cases, PAO and MO based grease, the level of removal varied most by method. The statistical significance of removal was evaluated with a Mann–Whitney rank sum test and is shown in Figure 13. For both the PAO and MO cases, UAS cleans better than water alone and the difference is statistically significant. There is also a statistically significant increase in cleaning when comparing the use of UAS with a degreasing agent to the use of degreasing agent alone.

For the mineral oil based lubricant (Figure 14), the difference between the UAS cleaning and water alone was statistically significant whereas the difference between water and added DA was not. The combination of UAS and DA was significantly more than Water or Water and DA by a P value of less than 0.01.

Optical measurements

The optical measurements give a slightly different picture. Figures 15 and 16 compare the different removal assessments for the PAO and mineral oil based lubricants, respectively. For the PAO grease, the volume removal is comparable to the mass removal as shown in Figure 15. When UAS is used, the amount of area that is fully cleaned is much greater, proportionally, than the mass or volume removed. This is because the

bubbles cleaning the surface get under the lubricant layer and shift the lubricant, causing clean patches with no lubricant and ridges where the thickness of the lubricant increases. The shifting of the lubricant is supported by the thickness measurements. The MO based lubricant (Figure 16) does not show this relation, which indicates that the bubbles were not able to get under the lubricant as effectively for this material.

Discussion and Conclusions

The relative cleaning performance of using UAS to remove lubricant was compared against a water rinse and the use of a DA. Four experimental conditions were tested: water rinse, UAS rinse, water rinse plus DA, UAS rinse plus DA. The mass before and after treatment was compared to evaluate the methods. For the two lubricants that showed the most sensitivity to testing imaging tests were conducted to measure the volume and area cleaned under the four conditions.

For two of the four lubricants, UAS provided a statistically significant improvement to lubricant removal and no cases showed a detrimental impact on cleaning. For the PAO grease, UAS was able to remove a higher percentage by area than by mass or volume. It is expected that a larger area is cleaned because the bubbles get under the lubricant layer and move the lubricant. Overall, UAS proved an effective method for lubricant removal: the forces of shear and microstreaming have been shown to be capable of removing lubricants 24 hours post application from stainless steel.

In terms of metal finishing, the possibilities go beyond cleaning. In addition to having the potential to clean a surface prior to electrodeposition, the ultrasonic stimulation of surface waves on a gas bubble during electrodeposition has been shown to enhance the electrodeposition current by generating mixing in the electrolyte through the action of the microcirculation currents that the surface waves induce, breaking down the

tendency to form a depletion layer in the electrolyte close to the electrode, leading to a qualitative difference in the pattern which copper was deposited [59].

That said, however, the primary importance of the UAS technology to metal finishing will probably be in cleaning: given the removal of industrial lubricants from stainless steel in this paper, it is likely that UAS technology has potential benefits for many industrial surface preparation processes, including welding, bonding and finishing, notably via cleaning that does not induce micro-scratches and so promote later contamination, wear and corrosion.

However, the current COVID-19 epidemic is a reminder that cleaning can have vital importance. As yet there is no specific treatment or preventive vaccine for COVID-19 and development of medication or immunisation may take more than a year. Control of the epidemic is by interrupting the transmission of virus to susceptible individuals.

Respiratory droplet spread infections are transmitted directly from patient to patient or indirectly from virus in respiratory secretions that settle on hard surfaces where the agent may remain infectious for prolonged periods of hours to days [60-62]. Illnesses with other modes of transmission such as blood or body fluids may also transmit via hard surfaces.

In other work, we have shown that this technology can remove bacteria [20, 21] and fungi (unpublished) from hard surfaces. Viruses, such as SARS-CoV-2, lack effector mechanisms and do not themselves attach to ordinary surfaces in distinction from bacteria that have complex adhesion mechanisms. Viruses only attach to specific receptors on cell surfaces; in the case of SARS-CoV-2, the ACE 2 receptors to which the virus attaches are found predominantly in lung tissue. The virus is contained in respiratory secretions which dry over time. Removing the virus by cleaning the surface of the respiratory secretions will interrupt the transmission of the disease.

We have previously demonstrated that this technology will remove prion protein infected brain homogenate that has dried onto surgical instruments [20]. Although the precise nature and rheology of the viscous liquid in which the virus exists may be different from normal respiratory secretions [63], they share many of the same components.

We have also shown previously that the technology will remove bacterial biofilm from a variety of surfaces including hands and hard surfaces [20, 21] . The effective tackling of biofilms using only sound, air and water meant that, unlike the use of conventional antimicrobial treatments (antibiotics, antivirals, antifungals etc.), the use of such technology did not so readily promote the rise of AntiMicrobial Resistance (AMR) [23, 24].

The importance of hand washing and cleaning of hard surfaces to prevent transmission of infection is well known. In the current epidemic, hand washing for 20 seconds with (warm) water and soap or rubbing with an alcohol-based hand sanitiser are recommended. Hard surfaces are cleaned with conventional or anti-microbial cleaners or wiped with a 70% solution of ethanol.

The severity of the disease is caused by the lack of both specific treatment options and a preventive vaccine. This is of course the case with all newly emerging infections, of which there have been a number in the last 20 years including Ebola, SARS, MERS and two new strains of influenza. There is no reason to suppose that more novel infections will not emerge in the coming years and the same issues of lack of treatment and vaccine will exist.

We will have to rely on traditional means of controlling epidemics which are independent of the causative organism. Isolation (quarantine) and social distancing are effective measures, but cleaning is known to be vital in reducing the transmission of the infectious agents. The continuing and large-scale use of cleaning agents is expensive, may

damage surfaces, particularly skin, and the supply is subject to disruption of the supply chain at many points. Different cleaning products are required for different surfaces. Manufacturing facilities may be overwhelmed, and the distribution services are not necessarily able to provide what is required when it is needed.

The importance of innovative cleaning technologies that use only water and electrical power (the bare minimum a hospital needs), cannot be over-stated. The UAS nozzle demonstrated here is independent of logistical support for its operation. It is equally effective against all current and possible viral illnesses transmitted from surfaces that have been contaminated by the airborne respiratory droplet route, or through other ways whereby contaminated surfaces can be an infection route.

Data Accessibility

All data supporting this study are openly available (with doi=10.5258/SOTON/D1325) from the University of Southampton repository at:
https://doi.org/10.5258/SOTON/D1325

Acknowledgements

The UAS device used was a Mark I StarStream (Ultrawave Ltd.). The support of Sloan Water Technology Ltd., Global-NAMRIP and Ultrawave Ltd. is acknowledged. Maryam Malakoutikhah is supported on an EPSRC Case studentship (project reference 1786155). The authors gratefully acknowledge support of the 2018 Royal Society's Lord Leonard and Lady Estelle Wolfson Foundation Translation Award which was used to fund equipment and consumables, and a pump priming award from the Medical Research Council Confidence in Concept scheme (MC_PC_17177 and MC_PC_16059), and pump-priming funding from the ESPRC grant NAMRA (EP/M027260/1). The authors are grateful to Dr Adam Wasenczuk and Dr Nicola Symonds for valuable contribtions on

discussing tha applicability of the technology to surface finishing.

Disclosure statement

No financial interest or benefit has arisen from the direct applications of this article. However the Principal Investigator (T.G.L.) is the inventor of the UAS nozzle used in the experimental work and is a Director and Inventor-in-Chief of the company (Sloan Water Technology, Ltd.) that owns his patents (Publication number: WO/2011/023746) and supported this research. Dr Dolder and Dr Zhu are employees of the company and the PhD student and first author, M. Malakoutikhah, is sponsored by that company and by an EPSRC CASE award (project reference 1786155).

References

[1] J. A. Morris: 'Energy Conservation in Metal Finishing', *Transactions of the IMF*, 1980, **58**, 106-108 pages, doi: 10.1080/00202967.1980.11870536.

[2] G. E. Hunt: 'Hazardous waste minimization: part IV waste reduction in the metal finishing industry', *JAPCA*, 1988, **38**, 672-680 pages, doi: 10.1080/08940630.1988.10466410.

[3] S. M. Muzakkir, H. Hirani, and G. D. Thakre: 'Lubricant for heavily loaded slow-speed journal bearing', *Tribology transactions*, 2013, **56**, 1060-1068 pages, doi: 10.1080/10402004.2013.823530.

[4] J. P. Davim, P. S. Sreejith, and J. Silva: 'Turning of brasses using minimum quantity of lubricant (MQL) and flooded lubricant conditions', *Materials and Manufacturing Processes*, 2007, **22**, 45-50 pages, doi: 10.1080/10426910601015881.

[5] C. T. Pinheiro, M. J. Quina, and L. M. Gando-Ferreira: 'Management of waste lubricant oil in Europe: A circular economy approach', *Critical Reviews in Environmental Science and Technology*, 2020, 1-36 pages, doi: 10.1080/10643389.2020.1771887.

[6] B. Daylan, N. Ciliz, and A. Mammodov: 'Hazardous process chemical and water consumption reduction through cleaner production application for a zinc electroplating industry in Istanbul', *Resources, conservation and recycling*, 2013, **81**, 1-7 pages, doi: 10.1016/j.resconrec.2013.09.002.

[7] M. C. Thornton, C. J. Newton, B. F. P. Keay, P. G. Sheasby, and J. T. Evans: 'Some surface factors that affect the spot welding of aluminium', *Transactions of the IMF*, 1997, **75**, 165-170 pages, doi: 10.1080/00202967.1997.11871166.

[8] R. Zheng, J. Lin, P. C. Wang, Q. Wu, and Y. Wu: 'Effects of a sheet metal stamping lubricant on static strength of adhesive-bonded aluminum alloys', *Journal of Adhesion Science and Technology*, 2015, **29**, 1382-1402 pages, doi: doi.org/10.1080/01694243.2015.1030908.

[9] C. Larson: 'Surface preparation and pretreatment prior to surface finishing', *Transactions of the IMF*, 2009, **87**, 6-7 pages, doi: 10.1179/174591909X399518.
[10] A. F. Averill, J. Ingram, and P. F. Nolan: 'Cleaning metal components after the Montreal Protocol—introductory review', *Transactions of the IMF*, 1998, **76**, 81-89 pages, doi: 10.1080/00202967.1998.11871200.
[11] T. G. Leighton: 'Bubble acoustics: from whales to other worlds', *In Proceedings of the Institute of Acoustics, Birmingham, UK*, 2014, 58-86 pages.
[12] T. G. Leighton: 'The acoustic bubble: Ocean, cetacean and extraterrestrial acoustics, and cold water cleaning', *Journal of Physics: Conference Series*, 2017, **797**, 23 pages, ISBN: 1742-6596, doi: 10.1088/1742-6596/797/1/012001.
[13] A. O. Maksimov and T. G. Leighton: 'Transient processes near the acoustic threshold of parametrically-driven bubble shape oscillations', *Acta Acustica united with Acustica*, 2001, **87**, 322-332 pages.
[14] A. O. Maksimov and T. G. Leighton: 'Pattern formation on the surface of a bubble driven by an acoustic field', *Proceedings of the Royal Society A: Mathematical, Physical and Engineering Sciences*, 2012, **468**, 57-75 pages, doi: 10.1098/rspa.2011.0366.
[15] T. G. Leighton: 'The Acoustic Bubble', 1994, Academic Press, London, San Diego, 640 pages, ISBN: 0124419208.
[16] A. O. Maksimov and T. G. Leighton: 'Acoustic radiation force on a parametrically distorted bubble', *The Journal of the Acoustical Society of America*, 2018, **143**, 296-305 pages, doi: 10.1121/1.5020786.
[17] T. G. Leighton: 'Cold water cleaning in the preparation of food and beverages: the power of shimmering bubbles', *Baking Europe*, Summer 2018, 24-28 pages.
[18] T. G. Leighton: 'Climate change, dolphins, spaceships and antimicrobial resistance: the impact of bubble acoustics', *Proceedings of the 24th International Congress on Sound and Vibration ICSV24, London, United Kingdom*, 23-27 July 2017, Editor: B. Gibbs, 6 pages, ISBN: 978-1-906913-27-4.
[19] L. R. Goodes, T. J. Harvey, N. Symonds, and T. G. Leighton: 'A comparison of ultrasonically activated water stream and ultrasonic bath immersion cleaning of railhead leaf-film contaminant', *Surface Topography: Metrology and Properties*, 2016, **4**, 6 pages, doi: 10.1088/2051-672X/4/3/034003.
[20] P. R. Birkin, D. G. Offin, C. J. B. Vian, R. P. Howlin, J. I. Dawson, T. J. Secker, R. C. Herve, P. Stoodley, R. O. C. Oreffo, C. W. Keevil, and T. G. Leighton: 'Cold water cleaning of brain proteins, biofilm and bone–harnessing an ultrasonically activated stream', *Physical Chemistry Chemical Physics*, 2015, **17**, 20574-20579 pages, doi: 10.1039/C5CP02406D.
[21] R. P. Howlin, S. Fabbri, D. G. Offin, N. Symonds, K. S. Kiang, R. J. Knee, D. C. Yoganantham, J. S. Webb, P. R. Birkin, T. G. Leighton, and P. Stoodley: 'Removal of dental biofilms with an ultrasonically activated water stream', *Journal of dental research*, 2015, **94**, 1303-1309 pages, doi: 10.1177/0022034515589284.
[22] M. Salta, L. R. Goodes, B. J. Maas, S. P. Dennington, T. J. Secker, and T. G. Leighton: 'Bubbles versus biofilms: a novel method for the removal of marine biofilms attached on antifouling coatings using an ultrasonically activated water stream', *Surface Topography: Metrology and Properties*, 2016, **4**, 10 pages, doi: 10.1088/2051-672X/4/3/034009.

[23] T. G. Leighton: 'Can we end the threat of anti-microbial resistance once and for all?', *Science in Parliament*, 2018, **74**, 29-32 pages.
[24] T. G. Leighton: 'To stop AMR once and for all: stop killing the bugs!', November 2017, Available: https://epsrc.ukri.org/blog/stopamr/
[25] E. Michaelides: 'Particles, bubbles & drops: their motion, heat and mass transfer', 2006, World Scientific, Singapore, 410 pages, ISBN: 9812566473.
[26] A. Aliseda and J. C. Lasheras: 'Effect of buoyancy on the dynamics of a turbulent boundary layer laden with microbubbles', *Journal of fluid mechanics*, 2006, **559**, 307-334 pages, doi: 10.1017/S0022112006000474.
[27] G. Vázquez, M. A. Cancela, C. Riverol, E. Alvarez, and J. M. Navaza: 'Application of the Danckwerts method in a bubble column: Effects of surfactants on mass transfer coefficient and interfacial area', *Chemical Engineering Journal*, 2000, **78**, 13-19 pages, doi: 10.1016/S1385-8947(99)00174-6.
[28] R. Kohli and K. L. Mittal: 'Developments in Surface Contamination and Cleaning, Vol. 1: Fundamentals and Applied Aspects', 2015, William Andrew, United States of America, 894 pages, ISBN: 0323312705, 9780323312707.
[29] J. Deng and T. Lee: 'Effect of ultrasonic surface finishing on the strength and thermal shock behavior of the EDMed ceramic composite', *International Journal of Machine Tools and Manufacture*, 2002, **42**, 245-250 pages, doi: 10.1016/S0890-6955(01)00109-2.
[30] S. B. Awad and R. Nagarajan: 'Chapter 6 - Ultrasonic cleaning', in Developments in Surface Contamination and Cleaning, 2010, Elsevier, 225-280, doi: 10.1016/B978-1-4377-7830-4.10006-4.
[31] K. L. Tan and S. H. Yeo: 'Surface modification of additive manufactured components by ultrasonic cavitation abrasive finishing', *Wear*, 2017, **378**, 90-95 pages, doi: 10.1016/j.wear.2017.02.030.
[32] P. R. Birkin, D. G. Offin, and T. G. Leighton: 'The study of surface processes under electrochemical control in the presence of inertial cavitation', *Wear*, 2005, **258**, 623-628 pages, doi: 10.1016/j.wear.2004.05.025.
[33] T. G. Leighton, W. L. Ho, and R. Flaxman: 'Sonoluminescence from the unstable collapse of a conical bubble', *Ultrasonics*, 1997, **35**, 399-405 pages, doi: 10.1016/S0041-624X(97)00014-0.
[34] T. G. Leighton, B. T. Cox, and A. D. Phelps: 'The Rayleigh-like collapse of a conical bubble', *The Journal of the Acoustical Society of America*, 2000, **107**, 130-142 pages, doi: 10.1121/1.428296.
[35] C. K. Turangan, G. J. Ball, A. R. Jamaluddin, and T. G. Leighton: 'Numerical studies of cavitation erosion on an elastic–plastic material caused by shock-induced bubble collapse', *Proceedings of the Royal Society A: Mathematical, Physical and Engineering Sciences*, 2017, **473**, 20170315 pages, doi: 10.1098/rspa.2017.0315.
[36] P. R. Birkin, D. G. Offin, and T. G. Leighton: 'Electrochemical measurements of the effects of inertial acoustic cavitation by means of a novel dual microelectrode', *Electrochemistry communications*, 2004, **6**, 1174-1179 pages, doi: 10.1016/j.elecom.2004.09.013.
[37] A. Jayaprakash, J. K. Choi, G. L. Chahine, F. Martin, M. Donnelly, J. P. Franc, and A. Karimi: 'Scaling study of cavitation pitting from cavitating jets and ultrasonic horns', *Wear*, 2012, **296**, 619-629 pages, doi: 10.1016/j.wear.2012.07.025.

[38] P. R. Birkin, D. G. Offin, C. J. B. Vian, and T. G. Leighton: 'Multiple observations of cavitation cluster dynamics close to an ultrasonic horn tip', *The Journal of the Acoustical Society of America*, 2011, **130**, 3379-3388 pages, doi: 10.1121/1.3650536.

[39] Z. W. Zhong and S. H. Gee: 'Failure analysis of ultrasonic pitting and carbon voids on magnetic recording disks', *Ceramics international*, 2004, **30**, 1619-1622 pages, doi: 10.1016/j.ceramint.2003.12.174.

[40] T. G. Leighton, P. R. Birkin, M. Hodnett, B. Zeqiri, J. F. Power, G. J. Price, T. Mason, M. Plattes, N. Dezhkunov, and A. J. Coleman: 'Characterisation of measures of reference acoustic cavitation (COMORAC): An experimental feasibility trial', in Bubble and particle dynamics in acoustic fields: modern trends and applications, 2005, Research Signpost, 37-94.

[41] T. G. Leighton: 'What is ultrasound?', *Biophysics and Molecular Biology*, 2007, **93**, 3-83 pages, doi: 10.1016/j.pbiomolbio.2006.07.026.

[42] T. G. Leighton, P. R. Birkin, and D. G. Offin: 'A new approach to ultrasonic cleaning', *Proceedings of the International Congress on Acoustics*, 2-7 June 2013, **19**, 4 pages, ISBN: 1939-800X, doi: 10.1121/1.4799209.

[43] P. R. Birkin, D. G. Offin, C. J. B. Vian, T. G. Leighton, and A. O. Maksimov: 'Investigation of noninertial cavitation produced by an ultrasonic horn', *The Journal of the Acoustical Society of America*, 2011, **130**, 3297-3308 pages, doi: 10.1121/1.3650537.

[44] T. G. Leighton, R. J. Lingard, A. J. Walton, and J. E. Field: 'Acoustic bubble sizing by combination of subharmonic emissions with imaging frequency', *Ultrasonics*, 1991, **29**, 319-323 pages, doi: 10.1016/0041-624X(91)90029-8.

[45] A. D. Phelps and T. G. Leighton: 'The subharmonic oscillations and combination-frequency subharmonic emissions from a resonant bubble: Their properties and generation mechanisms', *Acta Acustica united with Acustica*, 1997, **83**, 59-66 pages.

[46] T. G. Leighton, A. J. Walton, and M. J. W. Pickworth: 'Primary Bjerknes forces', *European Journal of Physics*, 1990, **11**, 47-50 pages.

[47] T. G. Leighton: 'Fluid loading effects for acoustical sensors in the atmospheres of Mars, Venus, Titan, and Jupiter', *The Journal of the Acoustical Society of America*, 2009, **125**, 214-219 pages, doi: 10.1121/1.3104628.

[48] S. D. Richards, T. G. Leighton, and N. R. Brown: 'Visco–inertial absorption in dilute suspensions of irregular particles', *Proceedings of the Royal Society of London. Series A: Mathematical, Physical and Engineering Sciences*, 2003, **459**, 2153-2167 pages.

[49] M. J. W. Pickworth, P. P. Dendy, T. G. Leighton, and A. J. Walton: 'Studies of the cavitational effects of clinical ultrasound by sonoluminescence: 2. Thresholds for sonoluminescence from a therapeutic ultrasound beam and the effect of temperature and duty cycle', *Physics in Medicine & Biology*, 1988, **33**, 1249-1260 pages, doi: 10.1088/0031-9155/33/11/003.

[50] M. J. W. Pickworth, P. P. Dendy, T. G. Leighton, E. Worpe, and R. C. Chivers: 'Studies of the cavitational effects of clinical ultrasound by sonoluminescence: 3. Cavitation from pulses a few microseconds in length', *Physics in Medicine & Biology*, 1989, **34**, 1139-1151 pages.

[51] T. G. Leighton: 'Transient excitation of insonated bubbles', *Ultrasonics*, 1989, **27**, 50-53 pages, doi: 10.1016/0041-624X(89)90009-7.

[52] T. G. Leighton, A. J. Walton, and J. E. Field: 'High-speed photography of transient excitation', *Ultrasonics*, 1989, **27**, 370-373 pages, doi: 10.1016/0041-624X(89)90036-X.
[53] F. Karaosmanoglu, G. Kurt, and T. Ozaktas: 'Long term CI engine test of sunflower oil', *Renewable Energy*, 2000, **19**, 219-221 pages, doi: 10.1016/S0960-1481(99)00034-8.
[54] ELECTROLUBE: 'Contact Lubricants Technical Data Sheet, Special Plastics Grease', 2 pages, Available: https://electrolube.info/pdf/tds/044/SPG.pdf
[55] ROCOL: 'Technical Data sheet: SAPPHIRE 2', 2 pages, Available: https://www.rocol.com/products/sapphire-2-high-performance--triple-life-bearing-grease-
[56] ROCOL: 'Technical Data sheet: SAPPHIRE Aqua-Sil', 2 pages, Available: https://www.rocol.com/products/sapphire-potable-water-bearing-grease
[57] C. W. Keevil: 'Nomarsky DIC microscopy and image analysis of bio-film', *Binary Comput. Microbiol.*, 1992, **4**, 93-95 pages.
[58] C. W. Keevil: 'Rapid detection of biofilms and adherent pathogens using scanning confocal laser microscopy and episcopic differential interference contrast microscopy', *Water Science and Technology*, 2003, **47**, 105-116 pages, doi: 10.2166/wst.2003.0293.
[59] D. G. Offin, P. R. Birkin, and T. G. Leighton: 'Electrodeposition of copper in the presence of an acoustically excited gas bubble', *electrochemistry communications*, 2007, **9**, 1062-1068 pages, doi: 10.1016/j.elecom.2006.12.025.
[60] S. M. Duan, X. S. Zhao, R. F. Wen, J. J. Huang, G. H. Pi, S. X. Zhang, J. Han, S. L. Bi, L. Ruan, and X. P. Dong: 'Stability of SARS coronavirus in human specimens and environment and its sensitivity to heating and UV irradiation', *Biomedical and environmental sciences: BES*, 2003, **16**, 246-255 pages. [Online]. Available: https://europepmc.org/article/med/14631830
[61] S. L. Warnes, Z. R. Little, and C. W. Keevil: 'Human coronavirus 229E remains infectious on common touch surface materials', *MBio*, 2015, **6**, e01697-15 pages, doi: 10.1128/mBio.01697-15.
[62] N. Doremalen, T. Bushmaker, D. H. Morris, M. G. Holbrook, A. Gamble, B. N. Williamson, A. Tamin, J. L. Harcourt, N. J. Thornburg, S. I. Gerber, J. O. Lloyd-Smith, E. Wit, and V. J. Munster: 'Aerosol and surface stability of SARS-CoV-2 as compared with SARS-CoV-1', *New England Journal of Medicine*, 2020, 3 pages, doi: 10.1056/NEJMc2004973.
[63] S. K. Lai, Y. Y. Wang, D. Wirtz, and J. Hanes: 'Micro-and macrorheology of mucus', *Advanced drug delivery reviews*, 2009, **61**, 86-100 pages, doi: 10.1016/j.addr.2008.09.012.
[64] D. G. Offin, P. R. Birkin, and T. G. Leighton: 'An electrochemical and high-speed imaging study of micropore decontamination by acoustic bubble entrapment', *Physical Chemistry Chemical Physics*, 2014, **16**, 4982-4989 pages, doi: 10.1039/C3CP55088E.

Figures

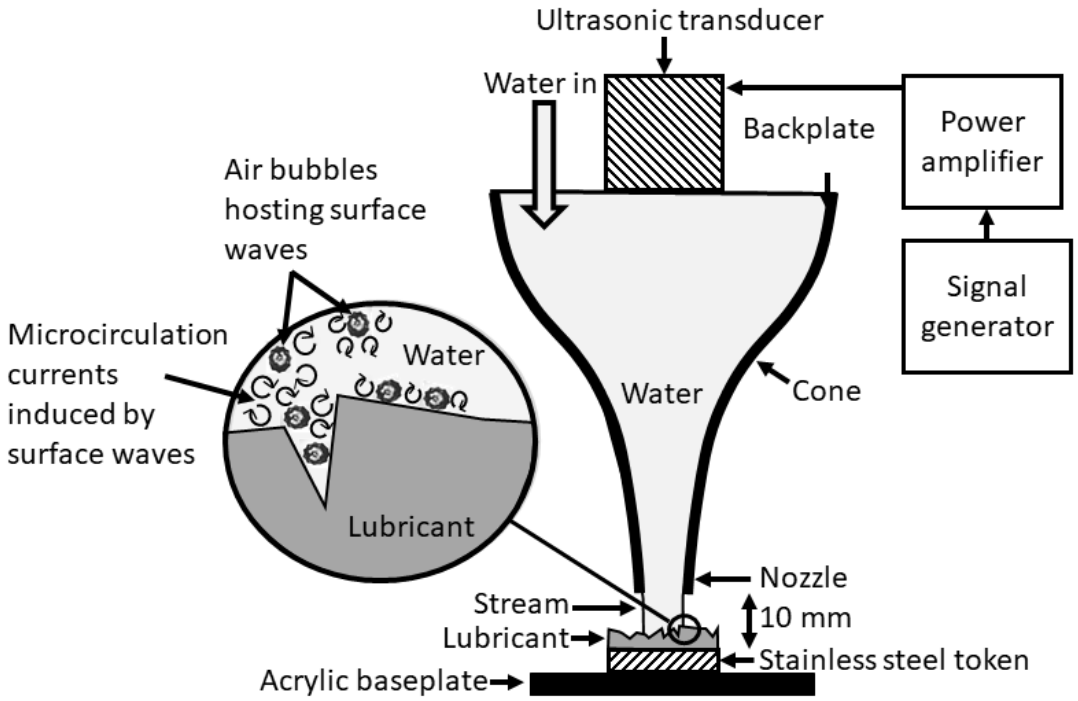

Figure 1: Schematic showing a stainless steel token covered with lubricant being cleaned by an Ultrasonically Activated Stream (UAS) nozzle. The inset magnifies a region where microscopic air bubbles, their walls rippling by ultrasonically-excited surface waves, clean away the lubricant using the microcirculation currents induced by the rippling surface waves.

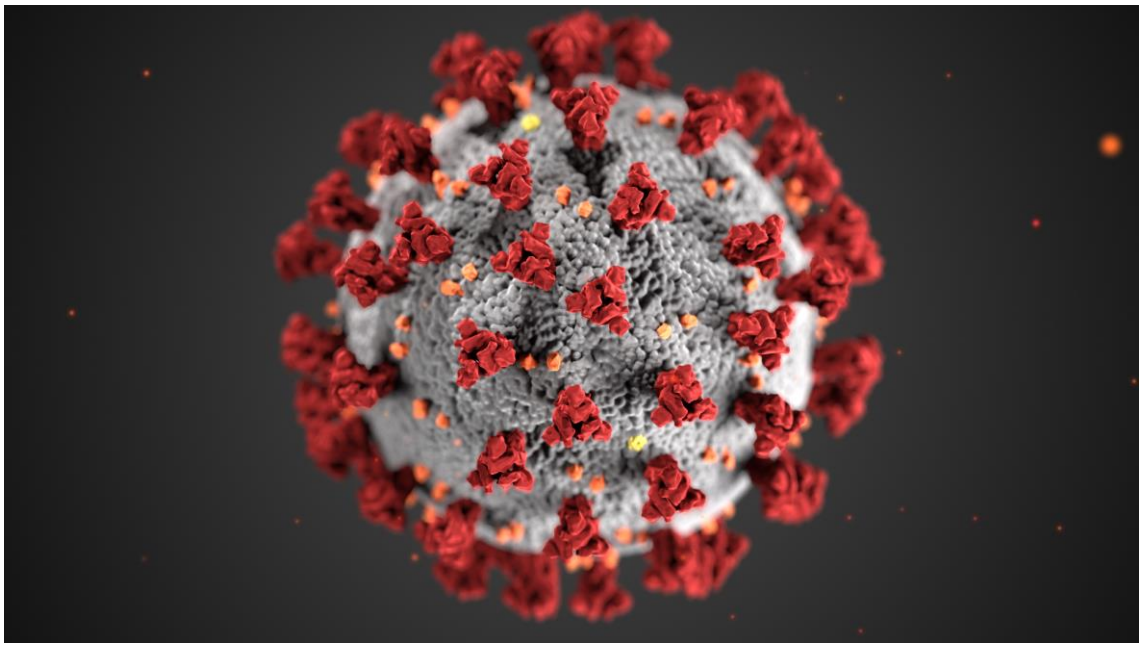

Figure 2. This illustration reveals ultrastructural morphology exhibited by coronaviruses. Note the spikes that adorn the outer surface of the virus, which impart the look of a corona surrounding the virion, when viewed electron microscopically. The coronavirus named Severe Acute Respiratory Syndrome coronavirus 2 (SARS-CoV-2) is a large virus (60-140 nm diameter) with a lipid envelope, and causes the illness named coronavirus disease 2019 (COVID-19). (Photo credit: Alissa Eckert, MS; Dan Higgins, MAMS. Image created in 2020 at the Centers for Disease Control and Prevention, CDC).

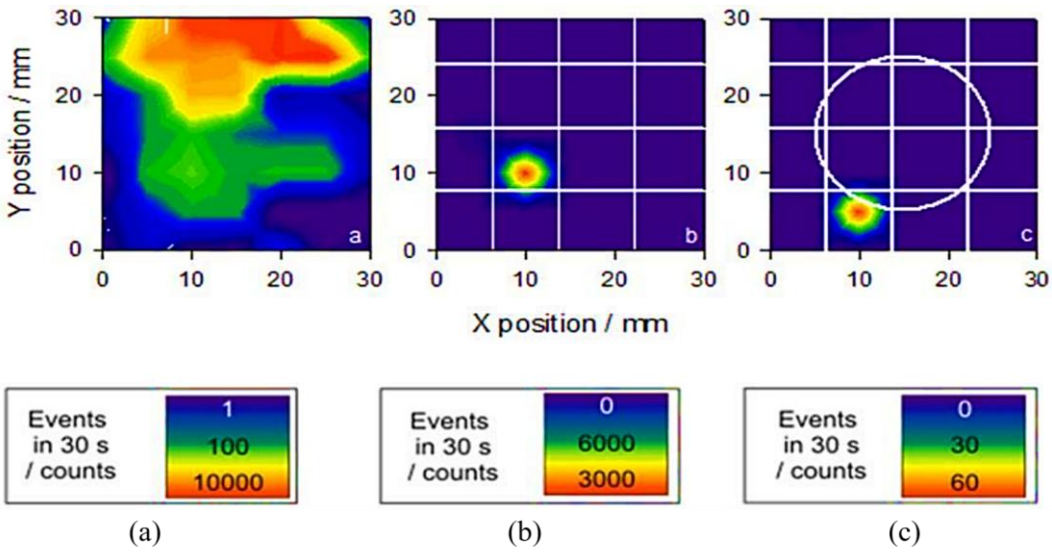

Figure 3: Inertial cavitation mapped over a 30 mm by 30 mm region in a commercial ultrasonic cleaning bath. (a) Before inserting the mesh tray supplied by the manufacturers to carry objects to be cleaned, the cavitation is inhomogeneous. (b) On inserting the tray into the field measured in (a), the cavitation is quenched over all of the map except for a new hot spot. (c) When a 1 pence UK coin is placed in the tray, there is further significant quenching (note the change in the scale for the counts of cavitation events per 30s): the hot spot moves and is significantly weaker (taken from Leighton et al. [17]).

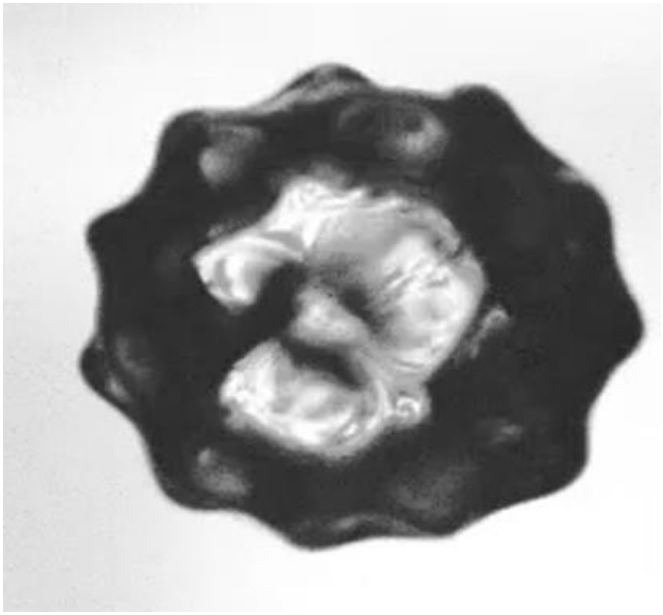

Figure 4: An image of an air bubble in water, hosting surface waves on the bubble wall stimulated by a driving acoustic field.

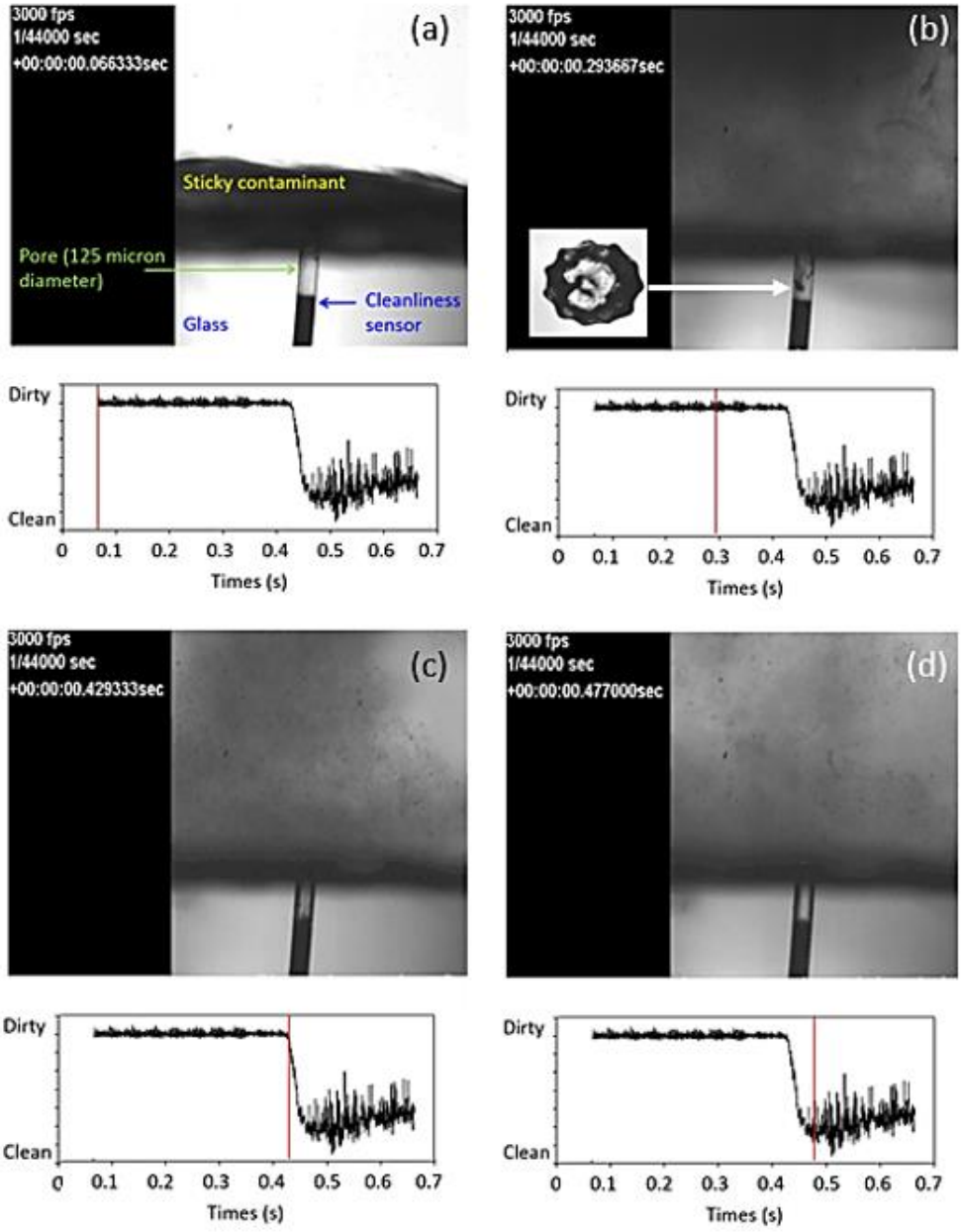

Figure 5: Four frames taken from a high speed movie filmed at 3000 frames per second Each panel [(a) to (d)] shows, in the upper half, the movie frame, and in the lower half of each frame is the output of a Platinum 'cleanliness sensor' which is placed at the base of a cylindrical pore (of diameter 125 microns) in the glass. For the artificial conditions of this visualization, the water is doped with chemicals that play no role in the cleaning (detailed in Ref. [64]). The expanded bubble in panel (b) is for figurative purposes and is not an actual magnification of the bubble in the pore at that time. See text for details. (taken from Leighton et al. [17]).

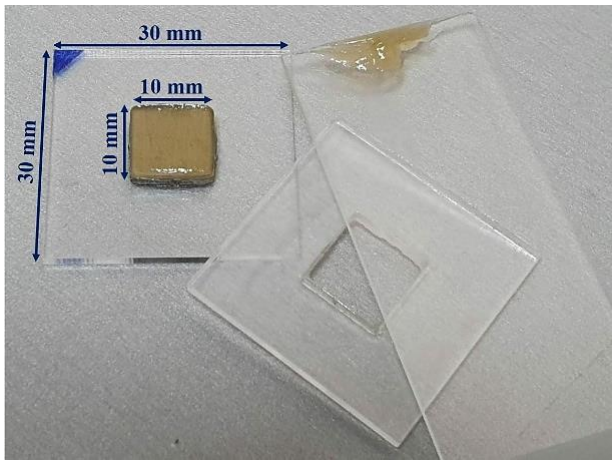

Figure 6: To deposit a thin layer of lubricant on top of the stainless steel token, it is first bonded to a baseplate of acrylic (shown on left), a template with a square cut-out (shown in middle) is placed around the metal. A layer of lubricant is placed on top of the cleaning sample and smoothed by a glass slide (shown on right), then the acrylic template plate is removed and the token is left covered by lubricant (shown on left).

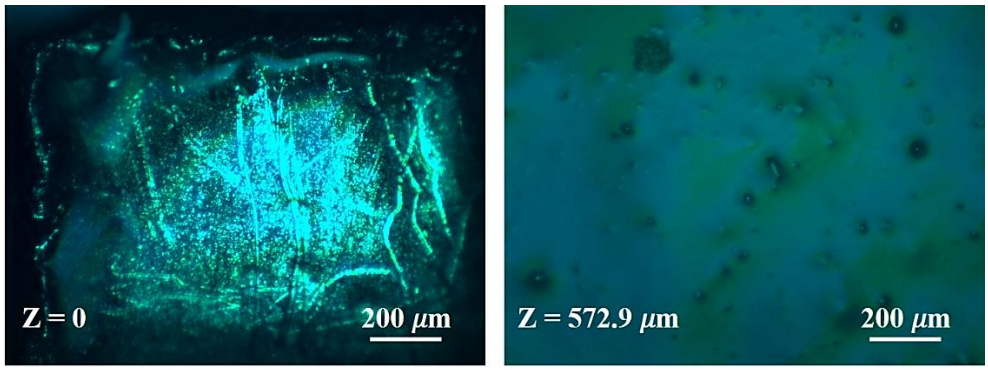

(a) (b)

Figure 7: Examples from a set of 80 microscope images (measuring 1340 μm×1000 μm) that are stitched together to form the images in each panel of Figure 8. This region of the coupon is shown when (a) focused on a section free from lubricant, and (b) focused onto the lubricant surface (in this image PAO grease). The electronic repository of this paper contains the original microscopic images, showing full detail.

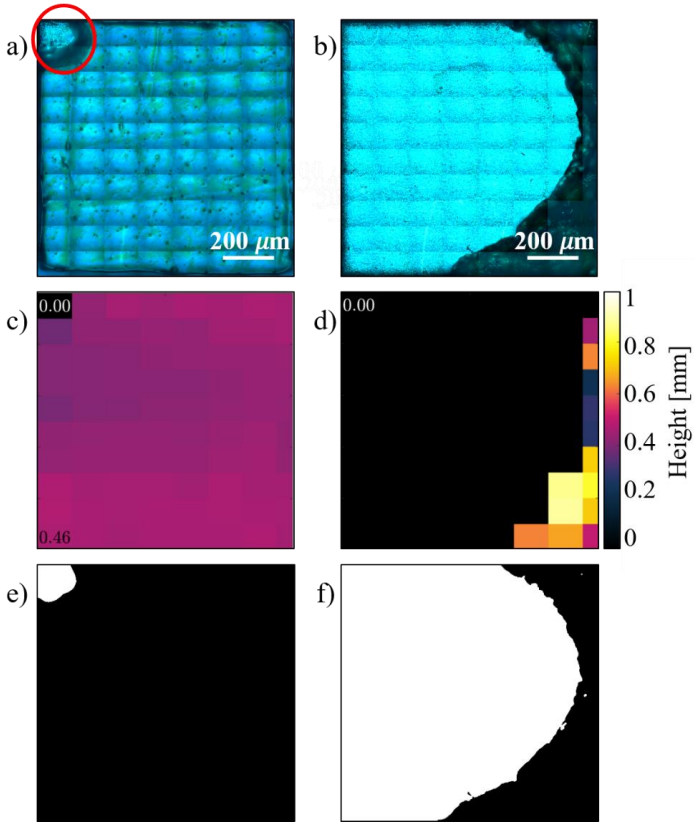

Figure 8: Panels (a) & (b) show combined photographs taken using the microscope (a) before and (b) after cleaning a token contaminated with PAO grease. Panels (c) and (d) show the heights recorded from the samples shown in (a) and (b), respectively. Panels (e) and (f) show thresholded images of the pictures shown in poanels (a) and (b) respectively, where cleaned surfaces are portrayed as white. All images are cropped to the 10 mm by 10 mm extent of the tile. The degreasing agent was applied 30 minutes prior to washing the token with UAS enhancement. The electronic data repository of this paper contains the original microscopic images, showing full detail.

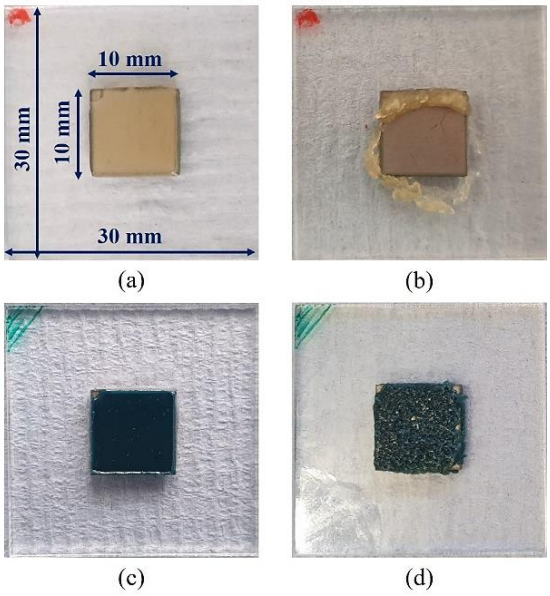

Figure 9: Examples of images amples of tokens before (a & c) and after (b & d) UAS cleaning. This is for both types of greases which were measured by the optical method (one example with degreaser, one without). (a) PAO grease before cleaning; (b) PAO grease after UAS cleaning without degreaser; (c) MO grease before cleaning and before the degreaser is applied; and (d) MO grease after UAS cleaning, which occurred 30 minutes after the application of degreaser. Note that in panel (b) the grease is displaced onto the acrylic surround.

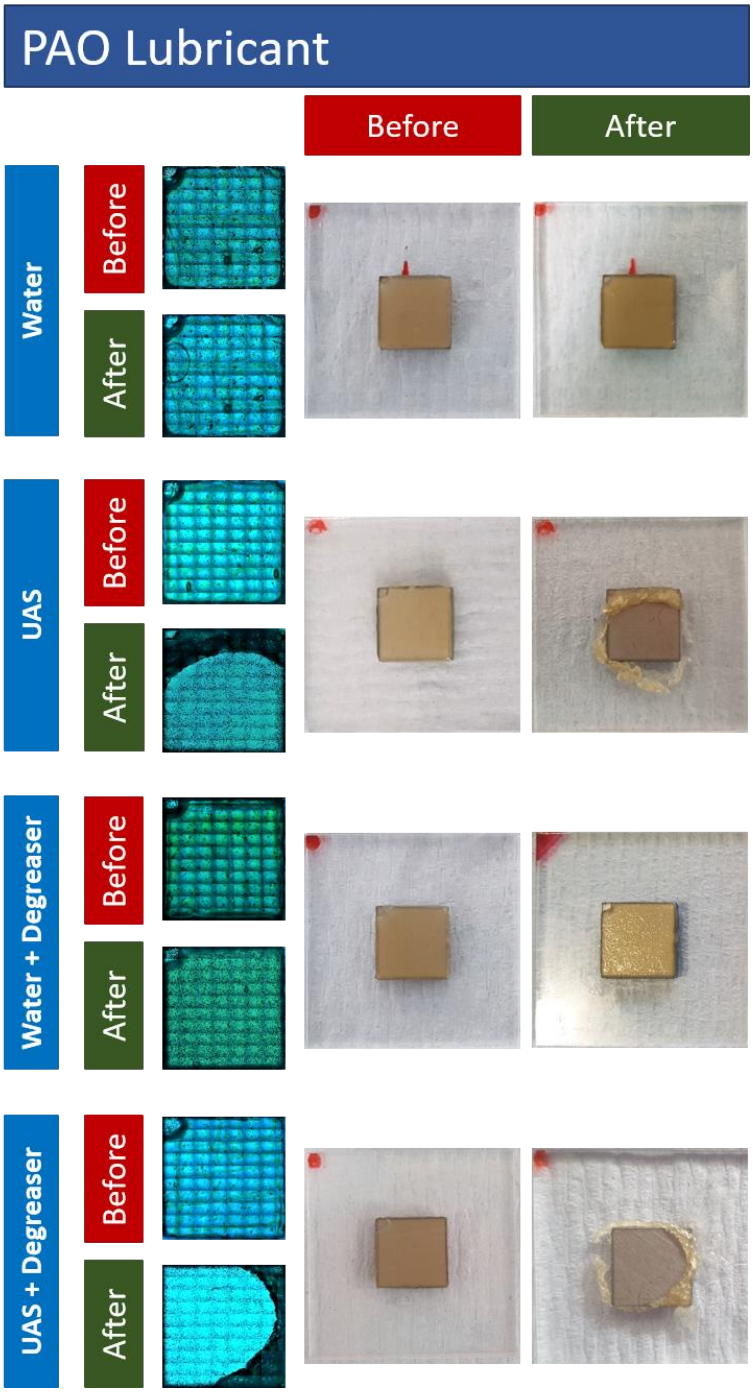

Figure 10: ‘Before-and-after’ high-resolution microscope images, stacked to form a large composite image on the left, are compared with ‘before-and-after’ photographic images (on the right) of PAO grease for the four possible cleaning conditions (as given by the label for each row on the left of the image). The electronic repository of this paper contains the original microscopic images, showing full detail.

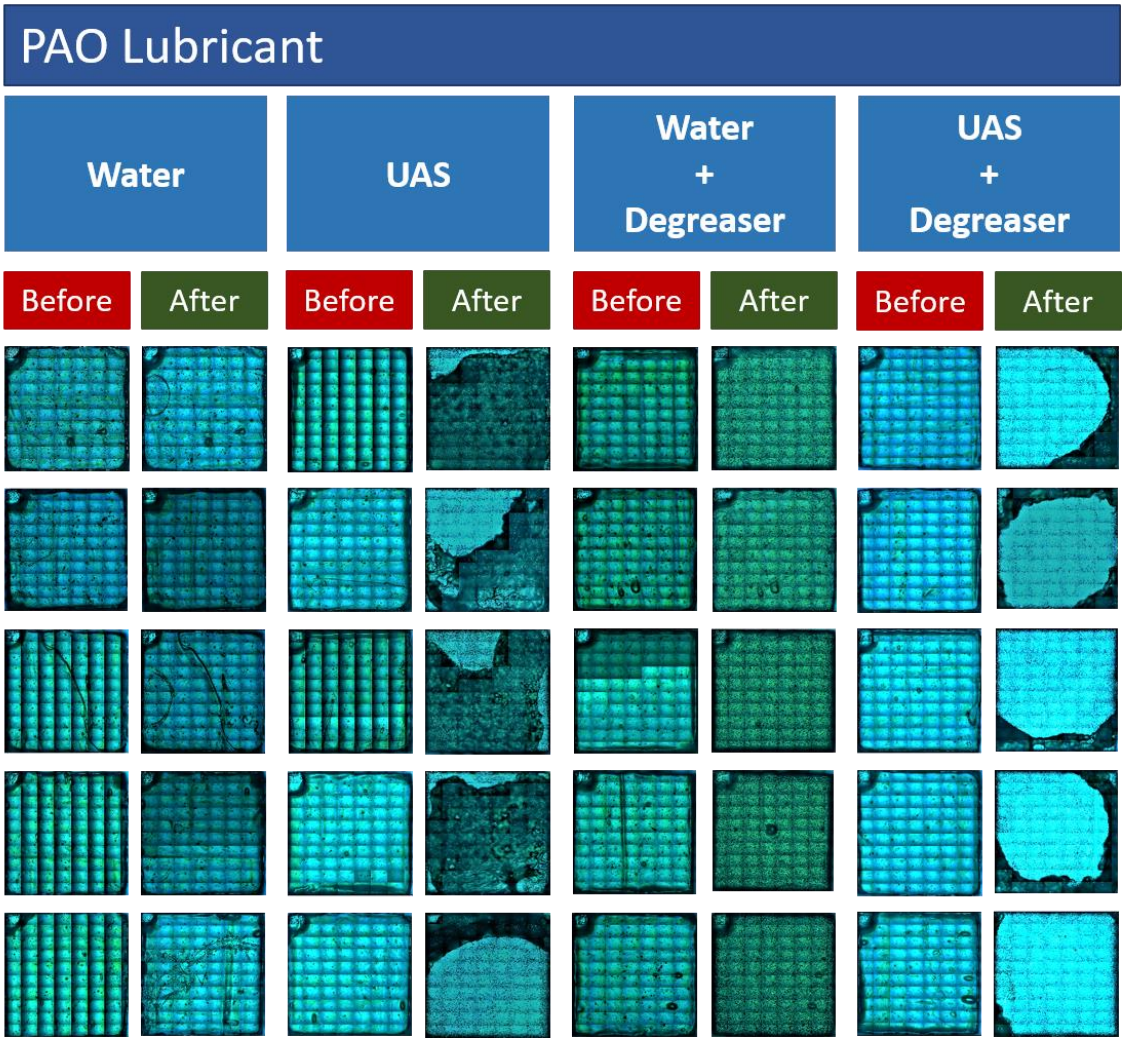

Figure 11: ‘Before-and-after’ high-resolution microscope images, stacked to form a large composite image, of PAO grease for the four possible cleaning conditions (as given by the label for each column at the top of the image). The electronic repository of this paper contains the original microscopic images, showing full detail.

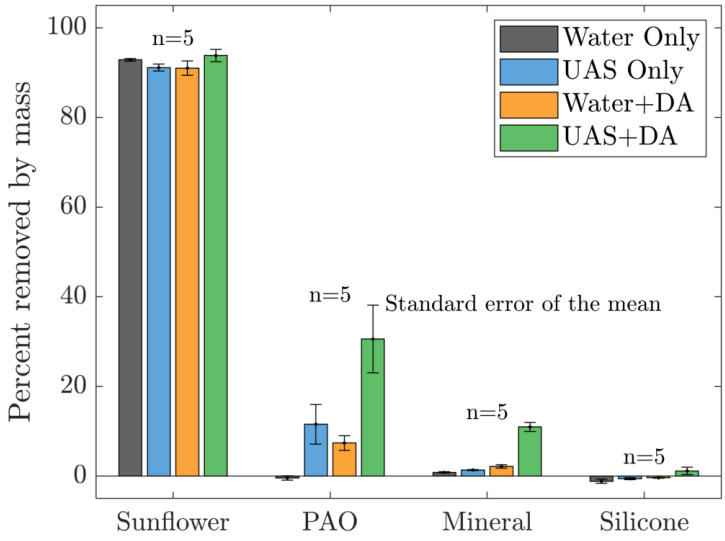

Figure 12: Percentage mass removal for the four lubricants tested and the four removal methods

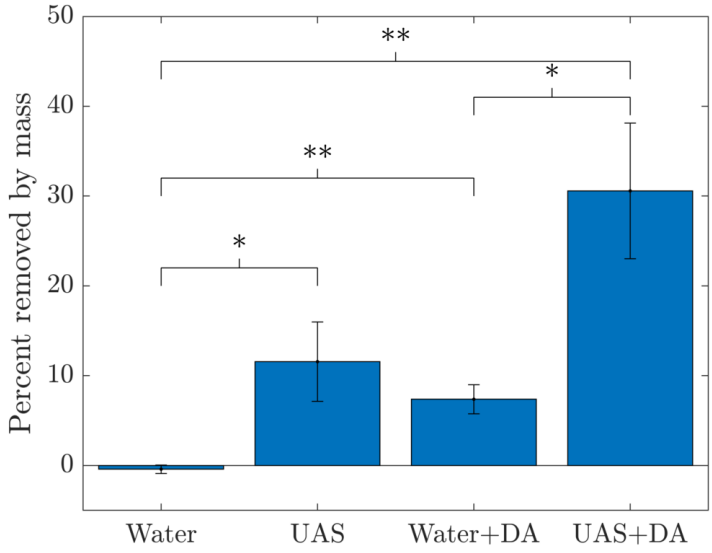

Figure 13: Statistical significance of different cleaning methods for PAO based grease over five tokens. The Mann−Whitney rank sum test was used where non-significance (NS) = $P > 0.05$, * = $P \leq 0.05$ and **= $P \leq 0.01$.

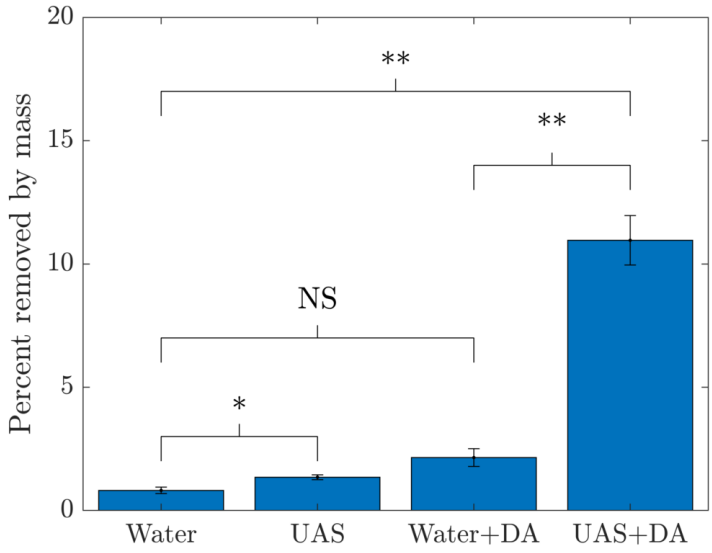

Figure 14: Statistical significance of different cleaning methods for mineral oil-based lubricant over five tokens. The Mann–Whitney rank sum test was used where non-significance (NS) = $P > 0.05$, * = $P \leq 0.05$ and ** = $P \leq 0.01$.

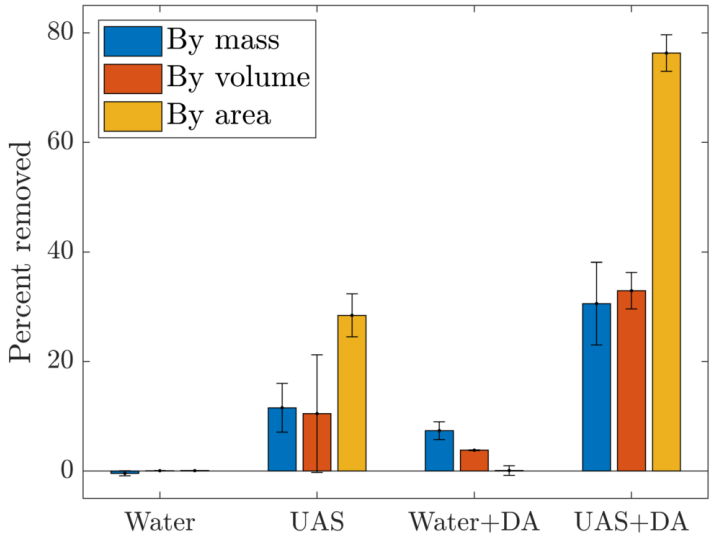

Figure 15: Removal of PAO grease measured by mass, volume, and area.

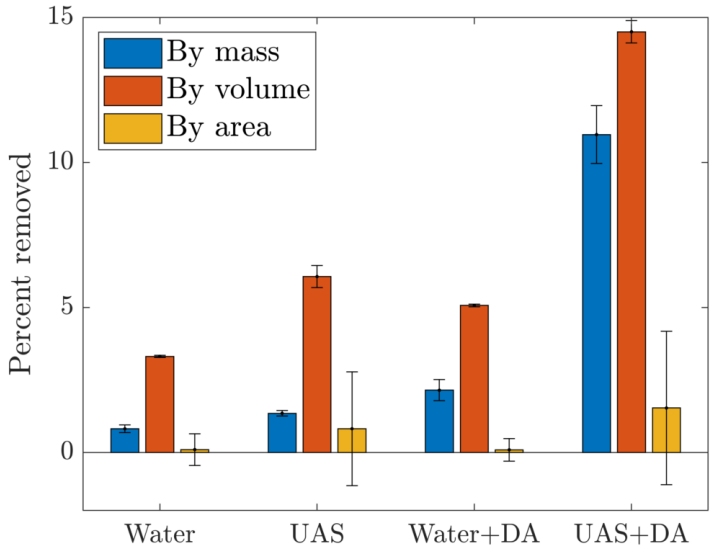

Figure 16: Removal of MO grease by mass, volume, and area.